Hindawi
Advances in Civil Engineering
Volume 2021, Article ID 3694838, 9 pages
https://doi.org/10.1155/2021/3694838

Research Article

Experimental Study on Axial Compression of an Insulating Layer through a Composite Shear Wall

Yuliang Wang, Congcong Wang, and Zhixing Cao

Tianjin Key Laboratory of Structural Protection and Reinforcement for Civil and Construction, Tianjin Chengjian University, Tianjin 300384, China

Correspondence should be addressed to Congcong Wang; wcc01172021@163.com

Received 11 April 2021; Revised 23 May 2021; Accepted 30 May 2021; Published 23 June 2021

Academic Editor: Xiuling Wang

Based on the research of composite walls at home and abroad, a construction method of continuous opening of the insulation layer in the specimen is proposed. In the edge component of the composite wall, the insulation layer should be thinned appropriately, the concrete on both sides should be thickened correspondingly, and U-shaped reinforcement should be used instead of stirrup. To study its axial compression test performance, five 1/2 scale composite shear wall specimens are tested under axial compression, including three composite wall specimens and two solid wall contrast specimens. The failure mode, load-bearing performance, deformation performance, and the collaborative work performance of wall are analyzed. The results show that the failure characteristics of the composite shear wall are similar to those of the solid wall, with splitting cracks at the corners and inverted triangular conical splitting at the top of the wall along the wall height direction, with no obvious bulging in the middle of the wall. The tie action of the ribs makes the concrete walls on both sides of the composite shear wall have good integrity and cooperative performance; the installation of the thermal insulation layer increases the overall thickness of the wall, improves the stability of the composite wall, and makes the composite wall axially compressed. The bearing capacity is not significantly reduced compared to the solid walls. Finally, according to the test results, the calculation formula of axial compression bearing capacity of composite shear wall is given, which provides the basis for the formulation of the code and engineering application.

1. Introduction

The composite shear wall (hereinafter referred to as composite wall) is a new type of wall which integrates thermal insulation and load-bearing. The wall is welded with steel grids on both sides by diagonal bars, sandwiched with thermal insulation materials in the middle, and poured with equal thickness concrete slabs on both sides. It has the advantages of good seismic performance and the same service life of the thermal insulation layer and building structure. At the same time, it can realize the transformation from building material fire prevention to building structure fire prevention and has good popularization and application prospects [1].

In foreign countries, the research on composite wall was carried out earlier, and Salmon et al. [2] carried out the comprehensive test and research on precast concrete sandwich panel. Ekenel and Tomlinson et al. [3, 4] conducted a comprehensive study on the connection mode of composite wall truss. Qin et al. [5] investigated a new type of double skin composite wall. And the influences of plate thickness on the structural performance were discussed in detail. Kisa et al. [6] carried out an experimental study on hysteretic behavior of steel plate composite shear walls and compared their energy dissipation, ductility, and stiffness performance according to the test results. Zhao et al. [7] analyzed the influence of two different restraint elements on the seismic performance and bearing capacity of shear walls from four aspects of the failure mode, hysteretic characteristics, stiffness, and residual deformation and calculated the equivalent lateral pressure. Yan et al. [8] studied the new EC connector of ultra-high performance concrete steel sandwich composite wall. Qin et al. [9] studied the experimental seismic performance of four newly designed double-

layer composite wall connections. Pan et al. [10] obtained that the shear bearing capacity of composite wall can be calculated according to the formula of "code for design of concrete structures" by testing the horizontal bearing capacity of steel wire grid cement fine aggregate sandwich panel. Li and Zhang et al. [11–13] studied the most basic mechanical properties of single wall under axial and eccentric compression and the seismic performance of composite wall. Huang et al. [14] conducted an experimental study on the seismic performance of middle and high-rise prefabricated composite walls. Chen et al. [15, 16] and others carried out the shear performance test and fire resistance research on cold-formed thin-walled steel bearing composite wall with sandwich panel cladding. Song et al. [17] carried out experimental research on seismic performance of thermal insulation composite shear wall. The composite wall structure with longitudinal stiffeners was studied in reference [18, 19]. Ye et al. [20, 21] studied the shaking table test and fire resistance of cold-formed steel composite shear wall.

To explore the possibility of the development of composite shear wall structure to high-rise and meet the national "four-step energy-saving" design standards, avoid the emergence of structural "heat bridge" and realize "building energy saving and structure integration" in the real sense. The existing composite wall structure form cannot meet these requirements. For this reason, 5 1/2 scale shear wall specimens are designed to test the axial compression performance of the composite wall by connecting the middle insulation layer of the composite wall and considering the structural measures such as increasing its thickness and replacing the stirrups of the edge members with U-shaped stirrups. The analysis of the failure process and failure pattern, bearing capacity, deformation performance, and wall cooperative performance are analyzed. The calculation formula of axial compression bearing capacity is put forward, which provides the basis for the theoretical research and engineering application of the composite wall.

2. Experimental Program

2.1. Specimen Design. The five composite wall specimens designed in this test are made in one batch. The 1/2 scale model is adopted, and the numbers are W1~W5, respectively. Among them, W1 and W2 are comparison specimens of reinforced grid solid shear wall and W3, W4, and W5 are the composite wall specimens. The basic parameters of the specimens are given in Table 1, and the design size and reinforcement of the specimens are shown in Figure 1. The reinforced concrete loading beam and the base beam are installed at the top and bottom of the specimen, respectively. The concrete cross-sectional area of the composite wall and solid wall are consistent. The clear height of the wall is 1500 mm and the width of the wall is 1000 mm. The length of the wall edge member is 200 mm, the longitudinal reinforcement of the edge member is 4Φ12, and the steel wire mesh is welded by cold-drawn low carbon steel wire with a diameter of 3.0 mm. Inclined steel wire is inserted to connect two pieces of steel mesh, which is used at the edge of the wall Φ6@100 U-bar instead of stirrups. The loading beam is 300 mm high, 300 mm wide, and 1100 mm long. The main reinforcement is 4Φ12, and the stirrup is Φ8 @ 100. The foundation beam is 400 mm high, 300 mm wide, and 1500 mm long. The main reinforcement is 4Φ16, and the stirrup is Φ8 @ 100. The self-compacting concrete is used as the concrete of the test piece, and the strength design grade is C30. The average cube compressive strength of the concrete is 38.4 MPa, and the mechanical properties of the reinforcement are given in Table 2.

2.2. Test Loading and Measurement. The axial compression specimens were loaded by a microcomputer-controlled electrohydraulic servo long column pressure testing machine. The test loading device is shown in Figure 2(a). When the specimen is installed in place, the fine sand layer is laid on the top and bottom surface to ensure the flatness of the loading surface. After the concrete structure is preloaded, the initial inelastic deformation can be eliminated to a certain extent, and whether all measuring instruments have entered the normal working state can be checked. The bulging deformation and out of plane deflection of the surface concrete of the test specimen under the action of axial pressure were measured by the resistance displacement meter with large gauge distance. In order to measure the axial compression displacement of the specimen, a displacement meter is arranged at the end of the loading beam on both sides. In order to measure the deflection of the specimen under axial compression during loading, a displacement meter is arranged at the middle of the structural layer on both sides of the specimen and at the upper and lower 1/4 height. At the same time, four displacement meters are arranged at both sides of the member to measure the lateral displacement of the member. The arrangement of the displacement meter is shown in Figure 2.

3. Results and Discussion

3.1. Crack Patterns. The main failure modes of the five shear walls are shown in Figure 3. From the analysis of the failure process and failure mode of the specimen, it can be seen that the crack development of the specimen is basically consistent in the stress process, and the stress characteristics can be divided into three stages:

(1) In the elastic stage, before the axial load reaches the cracking load, there is no obvious phenomenon in the wall, and the load-displacement curve is approximately linear. After the cracking load is reached, vertical cracks with a length of about 8 cm appear at the top corner of the wall on one side of W1 and W2. With the increase of the load, the microcracks on both sides of the wall increase, and the crack width also develops, about 0.1 mm~0.15 mm; W3, W4, and W5 along the wall height, there are many vertical cracks in the width range of the wall side, mainly concentrated in the width range of the insulation layer, continue to load, the vertical cracks in the insulation layer area are almost full along the

Table 1: Basic parameters of specimen.

Specimen name	The specifications of the wall			Wire mesh	U-shaped stirrup	Vertical bars of the edge restraint member	Reinforcement ratio (%)
	Type	Section size (mm × mm)	The wall thickness (mm)				
W1	The solid wall	1000 × 1500	80	50 × 50	Φ6@100	Φ12	0.353
W2	The solid wall	1000 × 1500	80	75 × 75	Φ6@100	Φ12	0.235
W3	The composite wall	1000 × 1500	40 + 50 + 40	75 × 75	Φ6@100	Φ12	0.235
W4	The composite wall	1000 × 1500	40 + 70 + 40	50 × 50	Φ6@100	Φ12	0.353
W5	The composite wall	1000 × 1500	40 + 70 + 40	75 × 75	Φ6@100	Φ12	0.235

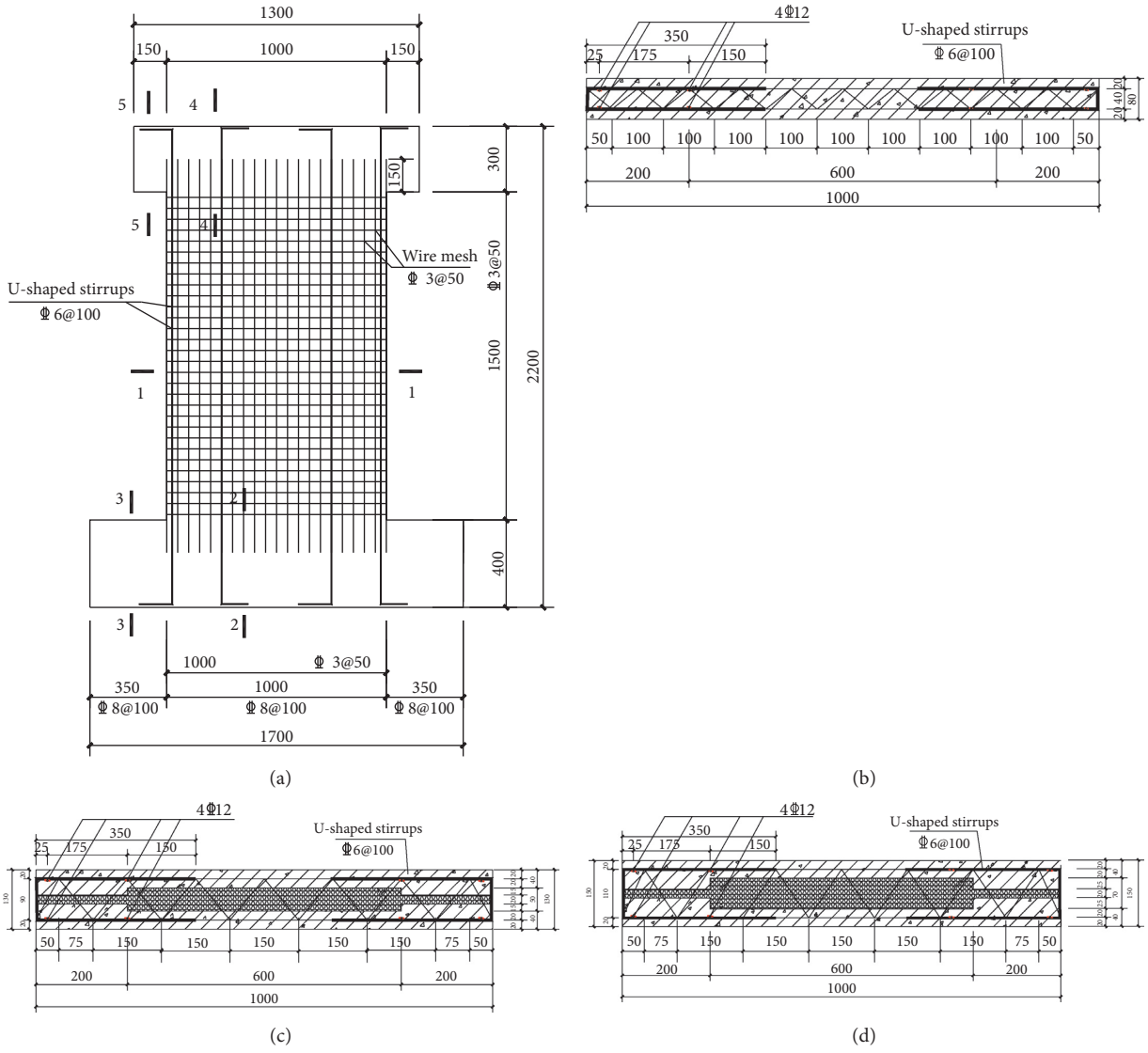

Figure 1: Dimensions and reinforcement details. (a) Elevation. (b) Section 1-1 of W1 and W2. (c) Section 1-1 of W3. (d) Section 1-1 of W4 and W5.

Table 2: Mechanical properties of reinforcement.

Nominal diameter d (mm)	Ultimate strength f_u (MPa)	Yield strength f_y (MP_a)	Modulus of elasticity E_s (GP_a)
3	593.3	396	210
6	573	523.5	200
12	471.2	410.4	200

(a) (b)

Figure 2: Arrangement of test loading device and displacement meter. (a) Test loading device. (b) Arrangement of the specimen displacement meter.

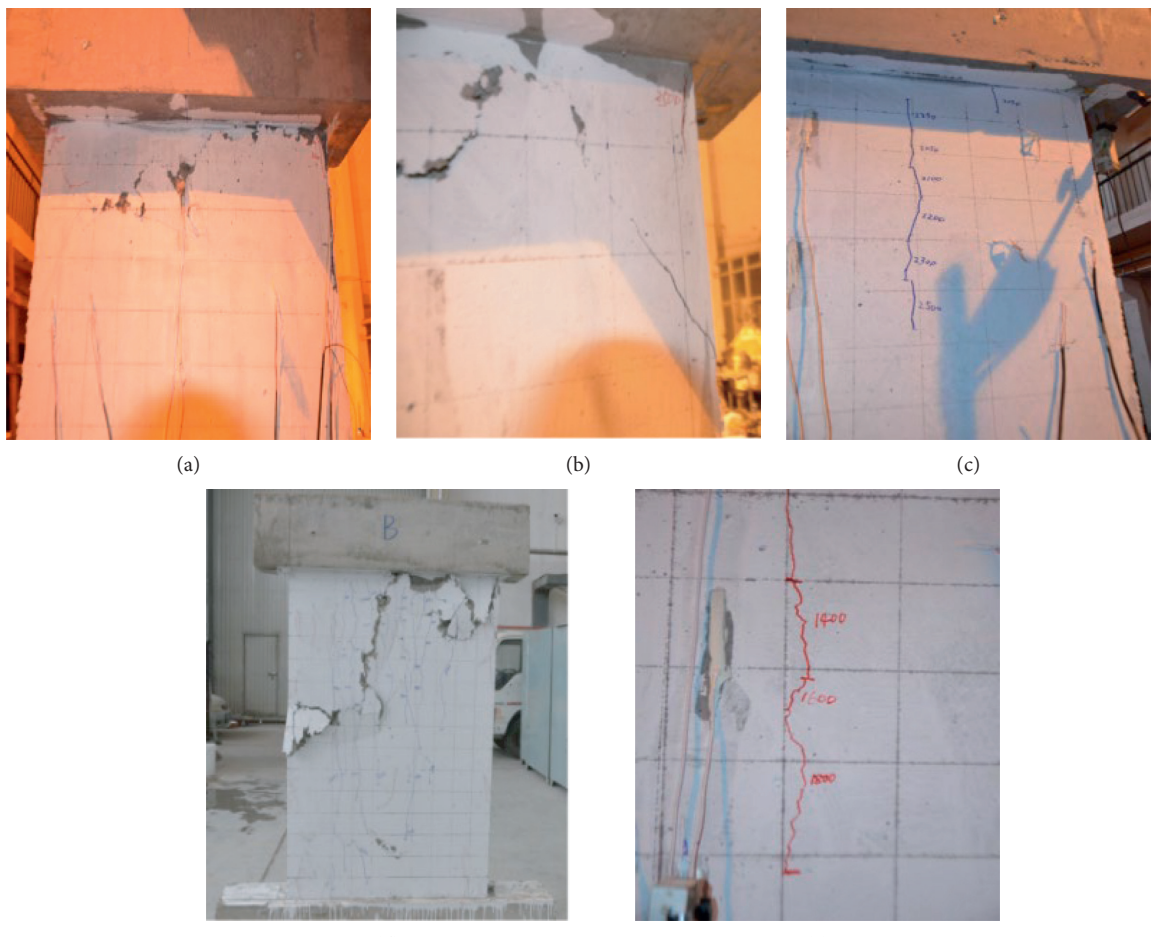

(a) (b) (c)

(d) (e)

Figure 3: Failure modes and crack distribution of all specimens. (a) W1. (b) W2. (c) W3. (d) W4. (e) W5.

direction of the wall height, and the width of the cracks in the insulation layer area is up to 0.15 mm.

(2) In the development stage, with the increase of axial vertical load, the lateral cracks of W1 and W2 walls increase and extend, and the width does not change significantly. The cracks in the structural layers on both sides of W3, W4, and W5 walls continue to extend to the bottom of the wall, and the width of the cracks continues to develop.

(3) In the failure stage, when the ultimate bearing capacity is reached, the final failure mode of W1 and W2 is the concrete peeling off the protective layer and some fall off. There is no damage phenomenon at the lower part, and the wall failure shows obvious

brittleness. When W3, W4, and W5 are damaged, the concrete at the junction of the loading beam and the wall are crushed, in the top corner of the wall appears a splitting crack, the top of the wall appears as an inverted triangle cone splitting along the direction of the wall height, and there is no obvious bulging phenomenon in the middle of the wall. The composite wall has a good cooperative working performance between various parts of the material.

3.2. Feature Point Data. The characteristic point data of each contrast specimen were obtained from the test and summarized as given in Table 3.

Through the comparison of W1, W2 and W3, W4, W5, it can be seen that the axial compression bearing capacity of the composite shear wall is not reduced by the removal of the solid wall into two equal thickness composite walls, and the reason is that the insulation layer is placed between the two sides of the wall, which increases the overall thickness of the wall, reduces the slenderness ratio of the wall, and improves the stability.

3.3. Load-Displacement Curve. The vertical compression displacement curves of the five specimens under axial uniform load are shown in Figure 4. Before the axial force reaches about 500 kN, the displacement of each specimen does not change obviously. With the increase of axial pressure, the relationship between displacement and load changes almost linearly until the wall is destroyed. There is no plastic horizontal section and descending section in the curve. The specimens are destroyed at the end of the elastic stage, and the compressive stiffness is very large.

3.4. Composite Wall Load-Deflection Curve. The lateral deflection curves of composite walls under uniformly distributed axial loads are shown in Figure 5. The reinforced concrete structural layers of the composite shear wall are connected to form a space truss by the diagonal bars, which are the stomach bars and only bear axial tension and compression. As can be seen from Figure 5, the lateral deflection curves of the structural layers on both sides of the three composite walls show a good trend consistency on the whole. The mechanical characteristics of the composite shear wall are when the axial load is small, the structural layers on both sides of A and B are in A small stress state, and the structural layers on both sides can bear the axial force separately, and the force of the cable-stayed reinforcement is not large. With the increase of axial force, the inflection point of the two structural layers begins to appear in the flexural diagram, which can be regarded as the cable-tensioning bars that start to play a better role in tying. At this time, the overall stiffness of the composite wall increases, and the lateral deflection of the composite wall increases at a slower rate than before after the inflection point. Therefore, the cable-stayed reinforcement has a great influence on the compression performance of the composite wall. Under the tension of the cable-stayed reinforcement, the structural layers on both sides can work together to resist the axial pressure and the compression ductility is also good.

3.5. Collaborative Working Performance of the Composite Wall. The test shows that the cooperative working performance of W3, W4, and W5 specimens is similar. Now take W5 as an example for analysis, as shown in Figure 6. Figure 6(a) shows the change of the strain of the main measuring points of the wire mesh along the horizontal position of the same structural layer with the axial pressure. With the increase of the uniform axial load, the strain trend of the grid reinforcement on the same section is relatively consistent. Before the axial load reaches 1000 kN, the strain curves of the grid reinforcement of the same section almost coincide. With the increase of the load, the difference of the strain of the grid reinforcement of the same section appears, which is caused by the stress concentration, and the position in the wall is most affected by the deflection. Figure 6(b) shows the strain variation trend of the longitudinal reinforcement at the edge of the same structural layer and the corresponding positions of the grid bars. With the increase of axial load, the strain trend of the two is consistent, which indicates that the edge longitudinal bars and the grid bars can work together well. Figure 6(c) shows the strain variation of the grid reinforcement at the corresponding positions of the concrete layers on both sides of the composite wall panels. With the increase of axial pressure, the strain of the steel bars on both sides of the grid is quite close, which indicates that the steel wires on both sides of the grid can cooperate with each other in deformation. The middle part is affected by the deflection most prominently, which leads to the difference of the section stress. Figure 6(d) shows the strain change trend of grid reinforcement and concrete at corresponding positions of structural layers on both sides of composite wall panel. With the increase of axial pressure, the strain changes of grid reinforcement and concrete in corresponding position are almost the same, and the steel mesh and concrete layer on both sides welded by inclined inserting wire can work well together. Figures 6(e) and 6(f) show the strain variation trend of the longitudinal reinforcement strain of the edge member and the steel wire grid along the height direction. With the increase of axial pressure, the strain change trend of steel wire mesh along the height direction is consistent with that of steel bar, which indicates that the edge longitudinal bar and steel bar mesh bound on the steel wire mesh have better cooperative ability.

3.6. Calculation of Axial Compression Bearing Capacity of Composite Wall. According to reference [11], the formula for calculating the axial compression bearing capacity of composite wall panels can be taken as the formula of solid wall in Code for Design of Concrete Structures (GB50010-2010). Considering the particularity of the composite wall structure, the reduction coefficient is adjusted. In this study, the reduction coefficient of 0.77, which is the same as that in reference [11], is adopted.

Table 3: Characteristic point data of comparison specimen.

Specimen name	Cracking load and corresponding strain value			The failure load and maximum strain value		
	Cracking load (kN)	Wire strain ($\mu\varepsilon$)	Concrete strain ($\mu\varepsilon$)	Failure load (kN)	Wire strain ($\mu\varepsilon$)	Concrete strain ($\mu\varepsilon$)
W1	1600	−829	−524	2350	−1900	−1303
W2	1800	−723	−500	2418	−2482	−1582
W3	1900	−672	−413	2530	−2134	−1400
W4	1400	−532	−400	2945	−2430	−1409
W5	1500	−590	−328	2680	−2856	−1300

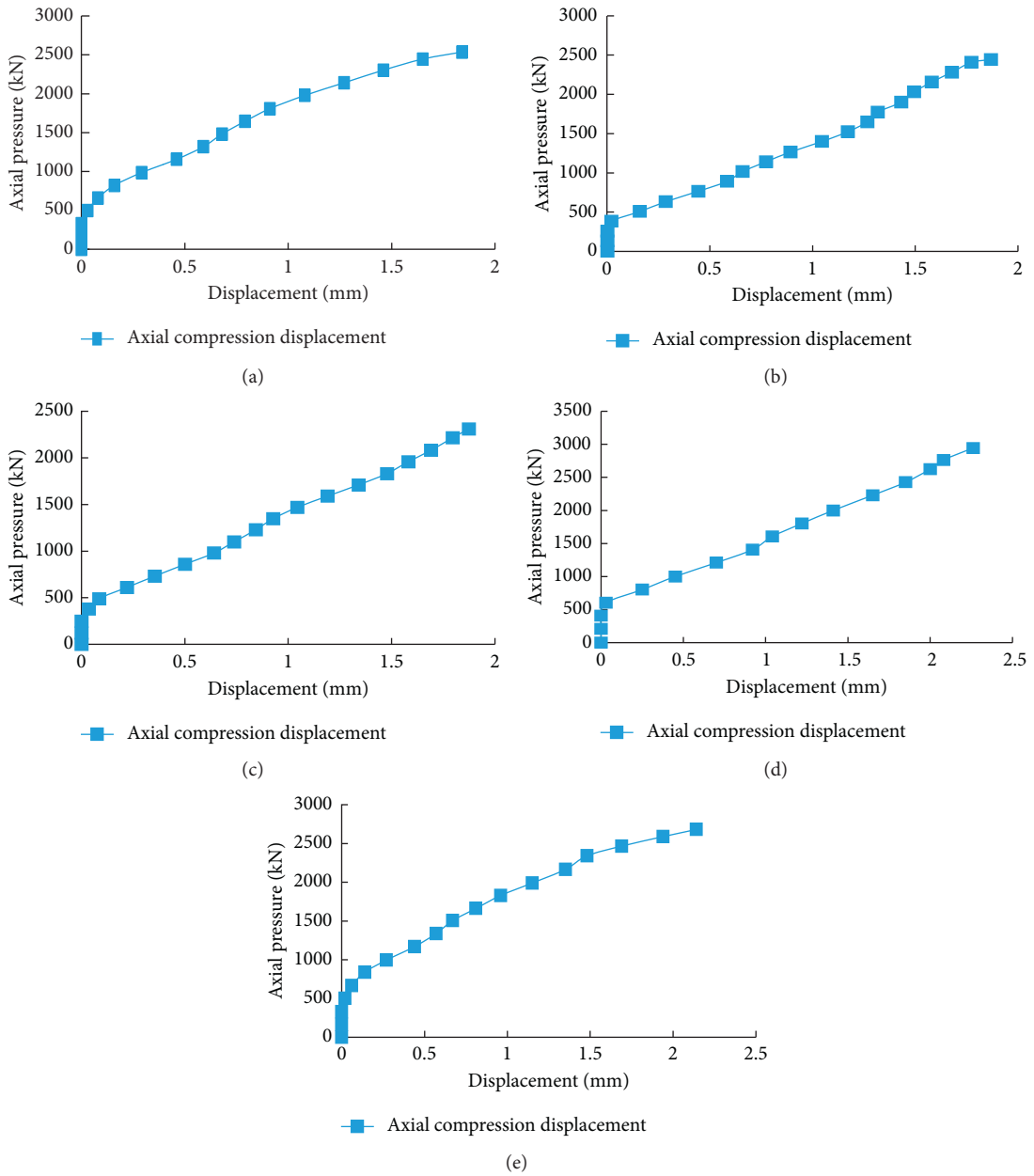

Figure 4: Load-displacement curve. (a) W1 specimen; (b) W2 specimen; (c) W3 specimen; (d) W4 specimen; (e) W5 specimen.

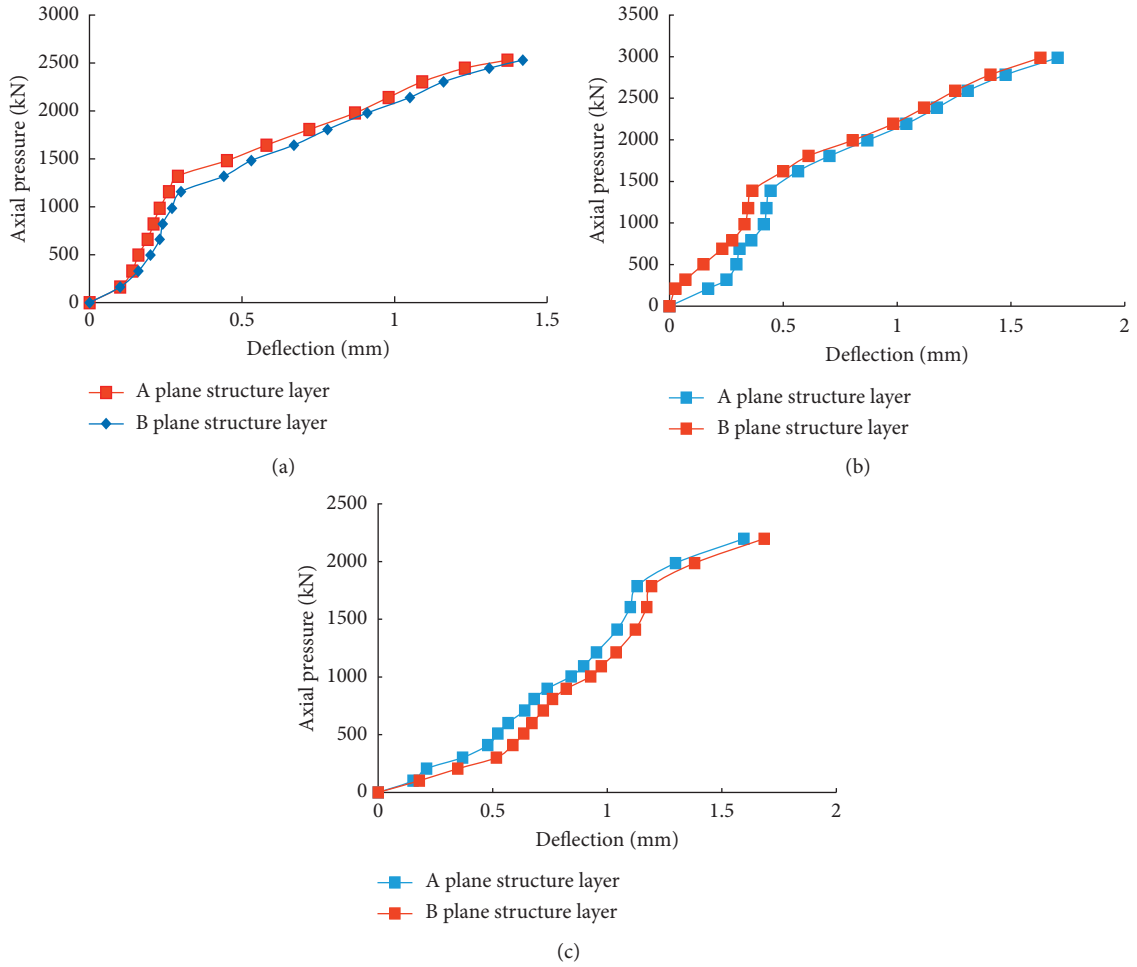

Figure 5: Load-deflection curve. (a) W3 specimen; (b) W4 specimen; (c) W5 specimen.

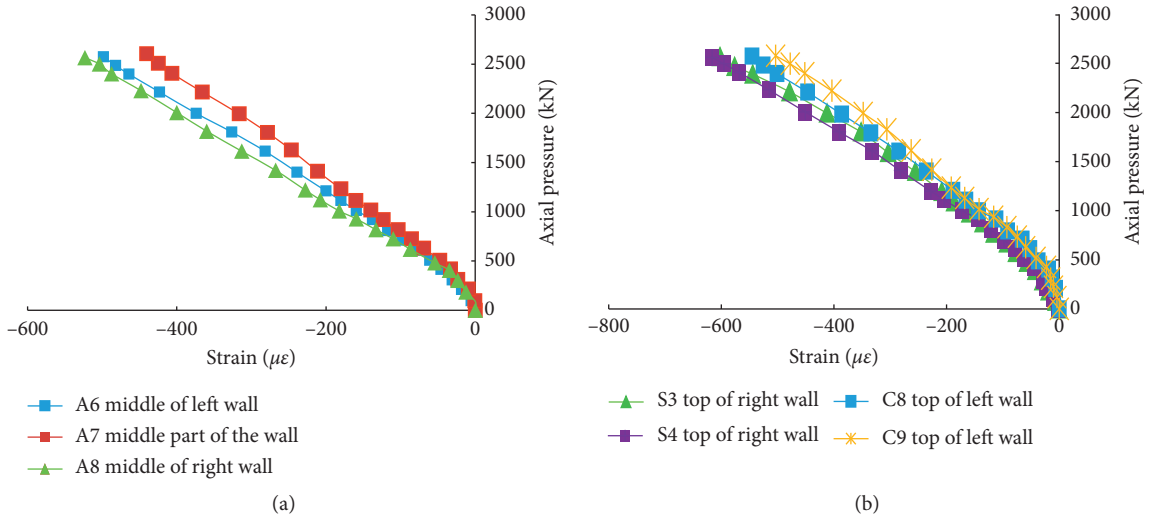

Figure 6: Continued.

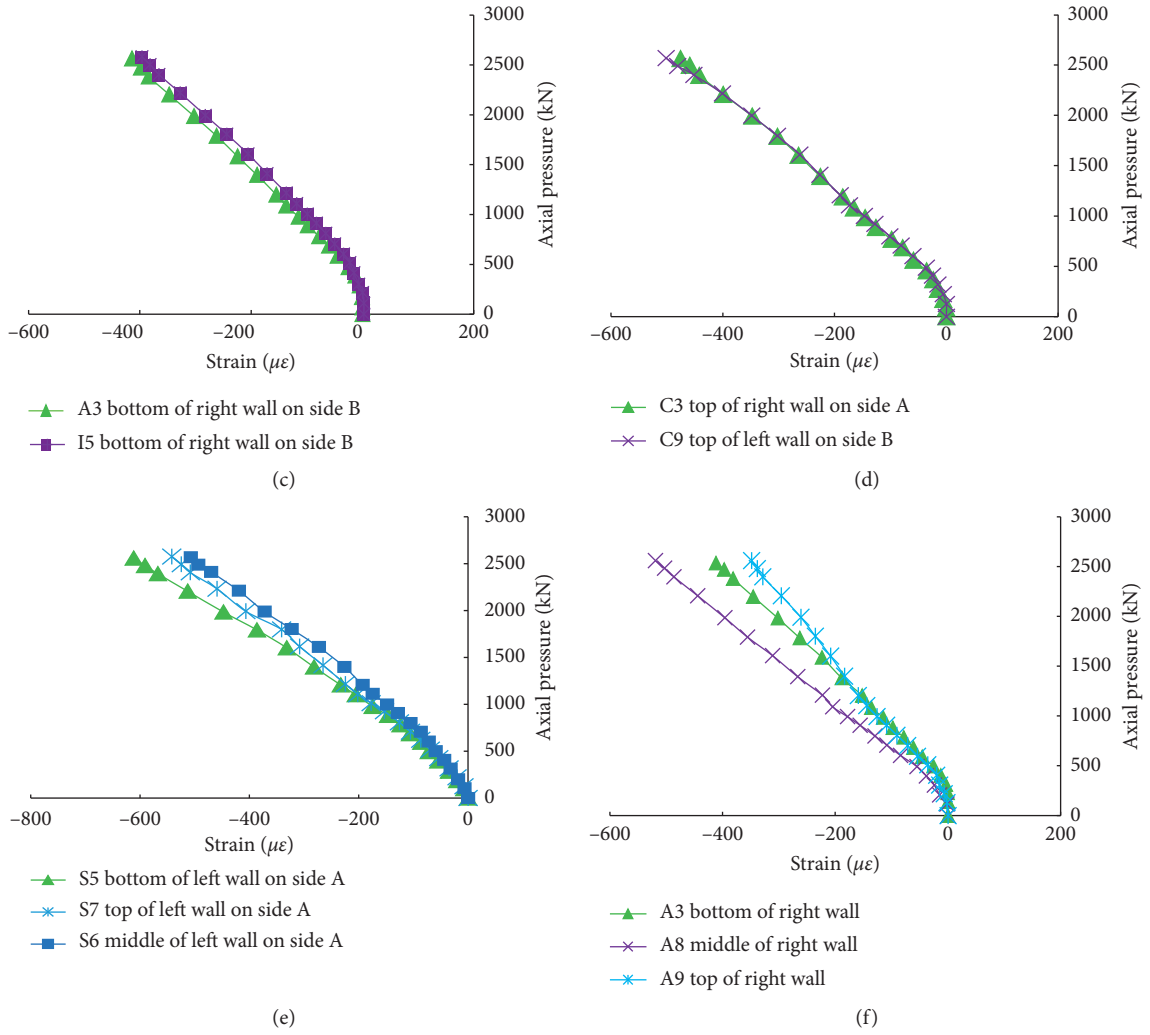

Figure 6: Strain variation of reinforcement. (a) Strain of the central grid reinforcement on the same side. (b) Strain of edge longitudinal bars. (c) Strain of grid reinforcement at corresponding positions on both sides. (d) Strain of grid reinforcement at corresponding positions on both sides. (e) Strain of edge longitudinal bars along the height. (f) Strain of grid reinforcement along height.

$$N_u = 0.77\varphi\left(f_c A + f_y' A_s'\right), \tag{1}$$

where N_u is the design value of axial pressure bearing capacity; 0.77 is the reduction factor; φ is the stability coefficient of reinforced concrete members under axial compression, and the wall thickness is the sum of the thickness of both sides of the wall sheet and the thickness of the insulation layer. f_c is the design value of axial compressive strength of concrete; A is the section area of member concrete; f_y' is the design value of compressive strength of longitudinal reinforcement; A_s' is the cross-sectional area of all longitudinal steel bars (including steel mesh reinforcement).

The comparison between the measured value and the calculated value of the axial compression bearing capacity of the composite wall is given in Table 4. The measured value of each wall is close to the calculated value of formula (1), and the ratio is greater than 1, which indicates that it can be used for the design and calculation of the axial compression bearing capacity of the composite shear wall.

Table 4: Calculation of bearing capacity of composite shear wall under axial compression.

Specimen number	Measured value (kN)	Calculated value (kN)	Measured value/ calculated value
W1	2350	1993	—
W2	2418	1967	—
W3	2530	2044	1.24
W4	2945	2121	1.39
W5	2680	2093	1.28

4. Conclusions

Through the axial compression test of composite shear wall, the failure mode of composite shear wall is preliminarily explored, and the axial compression performance of composite shear wall is analyzed. Based on the information presented in this study, the following conclusions can be drawn:

(1) The failure characteristics of composite shear walls are similar to those of solid walls. The top of the wall appears as an inverted triangular cone splitting along the height of the wall, and there is no obvious bulging phenomenon in the middle of the wall. The tie action of the bevel tension makes the concrete wall pieces on both sides of the composite shear walls have good integrity and cooperative working performance.

(2) The thermal insulation layer increases the overall thickness of the wall, improves the stability of the composite wall, and makes the axial compression bearing capacity of the composite wall not significantly lower than that of the solid wall.

(3) The calculation formula of axial compression bearing capacity of composite shear walls can adopt the basic form of the calculation formula of axial compression member bearing capacity stipulated in the Code for Design of Concrete Structures (GB 50010-2010), but the reduction coefficient in the formula should be changed to 0.77.

Data Availability

The data used to support the findings of this study are included within the article.

Conflicts of Interest

The authors declare that they have no conflicts of interest.

Acknowledgments

This work was supported by National Key R&D Program (2016YFC0701100), Tianjin Science and Technology Project (19YFZCSN01180), and Scientific Research Project of Tianjin Education Commission (2019ZD17).

References

[1] Y. H. Hao, H. Z. Xu, J. Q. Li, and Y. Wang, "Experimental study on axial performance of composite wall with interior insulation," *Journal of Building Structures*, vol. 36, no. S2, pp. 244–249, 2015.

[2] D. C. Salmon, A. Einea, and M. K. Tadors, "Full scale testing of precast concrete sandwich panels," *ACI Structure Journal*, vol. 94, no. 4, pp. 354–362, 1997.

[3] M. Ekenel, "Testing and acceptance criteria for fiber-reinforced composite grid connectors used in concrete sandwich panels," vol. 26, no. 6, https://www.researchgate.net/journal/Journal-of-Materials-in-Civil-Engineering-0899-1561, Article ID 06014004, 2013.

[4] D. G. Tomlinson, N. Teixeira, and A. Fam, "New shear connector design for insulated concrete sandwich panels using basalt fiber-reinforced polymer bars," *American Society of Civil Engineers*, vol. 20, no. 4, Article ID 04016003, 2016.

[5] Y. Qin, G. P. Shu, G. G. Zhou, and J. H. Han, "Compressive behavior of double skin composite wall with different plate thicknesses," *Journal of Constructional Steel Research*, vol. 157, pp. 297–313, 2019.

[6] M. H. Kisa, S. B. Yuksel, and N. Caglar, "Experimental study on hysteric behavior of composite shear walls with steel sheets," *Journal of Building Engineering*, vol. 33, Article ID 101570, 2020.

[7] N. N. Zhao, Y. H. Wang, Q. Han, and H. Su, "Bearing capacity of composite shear wall incorporating a concrete-filled steel tube boundary and column-type reinforced wall," *Advances in Structural Engineering*, vol. 23, no. 10, pp. 2188–2203, 2020.

[8] J. B. Yan, A. Chen, and T. Wang, "Compressive behaviours of steel-UHPC-steel sandwich composite walls using novel EC connectors," *Journal of Constructional Steel Research*, vol. 173, no. 6, Article ID 106244, 2020.

[9] Y. Qin, G. P. Shu, H. K. Zhang, and G. G. Zhou, "Experimental cyclic behavior of connection to double-skin composite wall with truss connector," *Journal of Constructional Steel Research*, vol. 162, 2019 in Chinese, Article ID 105759.

[10] P. Pan, J. R. Qian, Z. H. Pan et al., "Experimental study and simplified calculation method of prefabricated steel-mesh cement infilled panels," *Building Structure*, vol. 40, no. 4, pp. 41–43, 2010.

[11] S. C. Li, "Experimental investigation on composite wall panels under axial compression," *Journal of Huaqiao University*, vol. 27, no. 4, pp. 384–387, 2006.

[12] S. C. Li, "Research on restoring force model of composite walls with hidden frame," *Journal of Building Structures*, vol. 30, no. S2, pp. 74–79, 2009.

[13] T. Y. Zhang, M. Z. Wu, and Q. R. Yu, "Influence of axial pressure on the seismic property of sandwich wall panel," *Journal of Xi'an University of Architecture & Technology*, vol. 33, no. 2, pp. 127–130, 2001.

[14] W. Huang, M. Zhang, L. Song et al., "Experimental studies on seismic behavior of mid-highrise prefabricated composite walls," *Journal of Huazhong University of Science and Technology (Natural Science Edition)*, vol. 44, no. 12, pp. 56–63, 2016.

[15] W. Chen, J. H. Ye, and Y. Xu, "Shear experiments of load-bearing cold-formed thin-walled steel wall system lined with sandwich panels," *Journal of Building Structures*, vol. 38, no. 7, pp. 85–92, 2017.

[16] J. H. Ye and W. Chen, "Research progress on the fire resistance of cold-formed steel framed shear wall structures," *Journal of Building Structures*, vol. 19, no. 6, pp. 1–9+98, 2017.

[17] X. R. Song, C. L. Huang, D. H. Gao et al., "Experimental study on the seismic performance of thermal insulation composite shear wall," *Concrete*, vol. 41, no. 5, pp. 129–134, 2019.

[18] K. Wang, G. X. Chen, and R. Shan, "Dynamic response analysis of longitudinal reinforcement structure of rib composite wall," *World Seismic Engineering*, vol. 36, no. 1, pp. 77–84, 2020.

[19] G. X. Chen, Y. S. Chen, and X. M. Lv, "Study on seismic performance and influence factors of lateral stiffness of reinforced rib composite wall with a window," *World Seismic Engineering*, vol. 35, no. 1, pp. 27–35, 2019.

[20] J. H. Ye and L. Q. Jiang, "Hierarchical shaking-table tests of prefabricated mid-rise cold-formed steel composite shear wall buildings," *Journal of Building Structures*, vol. 41, no. 7, pp. 63–73, 2020.

[21] J. H. Ye and W. W. Chen, "Experimental study on fire resistance of full-scale cold-formed steel composite shear wall structure under real fire conditions," *Journal of Building Structures*, vol. 42, no. 6, 2020.